Journal of Power Sources 195 (2010) 1714–1719

Contents lists available at ScienceDirect

Journal of Power Sources

journal homepage: www.elsevier.com/locate/jpowsour

Anode performance of boron-doped graphites prepared from shot and sponge cokes

Tao Liu[a], Ruiying Luo[a,*], Seong-Ho Yoon[b,**], Isao Mochida[b]

[a] School of Science, Beihang University, Beijing 100083, China
[b] Institute for Materials Chemistry and Engineering, Kyushu University, Kasuga, Fukuoka 816-8580, Japan

ARTICLE INFO

Article history:
Received 4 August 2009
Received in revised form 29 August 2009
Accepted 31 August 2009
Available online 26 September 2009

Keywords:
Shot coke
Sponge coke
Boron-doped carbons
Graphitization
Electrochemical properties

ABSTRACT

The structures and anode performances of graphitized pristine and boron-doped shot and sponge cokes have been comparatively studied by means of scanning electron microscope (SEM), X-ray diffraction (XRD), X-ray photoelectron spectroscopy (XPS) and galvanostatic measurement. The results show that high degree of graphitization can be obtained by the substituted boron atom in the carbon lattice, and boron in the resultant boron-doped graphites mainly exist in the form of boron carbide and boron substituted in the carbon lattice. Both of boron-doped graphites from shot and sponge cokes obtain discharge capacity of 350 mAh g^{-1} and coulombic efficiency above 90%. Apart from commonly observed discharge plateau for graphite, boron-doped samples in this study also show a small plateau at ca. 0.06 V. This phenomenon can be explained that Li ion stores in the site to be void-like spaces that are produced by "molecular bridging" between the edge sites of graphene layer stack with a release of boron atoms substituted at the edge of graphene layer. The effect of the amount of boron dopant and graphitization temperature on the anode performance of boron-doped graphite are also investigated in this paper.

1. Introduction

Synthetic graphite has been well applied to the anodic material of commercial Li ion battery due to its large reversible capacity and long plateau in the low voltage [1–6]. It is usually prepared from graphitizable carbon such as needle coke, mesocarbon microbeads (MCMB) and mesophase pitch-based carbon fibers (MPCF) through graphitization above 2800 °C. Such high temperature heat-treatment incurs high cost in mass production.

It has been well established that, boron, as a graphitization catalyst, can enhance the graphitization of carbons. Thus, Boron doping can help graphitizable carbon obtain the high degree of graphitization under a lower graphitization temperature. Furthermore, boron doping can modify the electronic properties of the host carbon materials due to boron atom substituted for carbon atom in the carbon lattice [7–18]. Theoretically, the presence of boron should be beneficial for lithium intercalation/de-intercalation behavior of carbon material, because the substituted boron atom acts as an electron acceptor. Many studies on the boron doping into MCMB [10,11], MPCF [12–14] and pitch coke [15–17] have approved that boron doping can improve the discharge capacity and initial coulombic efficiency.

Shot and sponge cokes are byproducts of delayed coking operations that use petroleum feedstocks to produce valuable needle coke [19,20]. Both of them are anisotropic in nature. Shot coke is an undesirable product in the form of small spheres and no commercial application has been identified. Sponge coke can be used for fuel or to manufacture carbon anodes for electrolytic aluminum production. Therefore, compared with other currently used precursor materials, shot and sponge cokes are attractive in their low cost.

In this study, graphitized shot and sponge cokes and boron-doped graphites were characterized by X-ray diffraction (XRD) and X-ray photoelectron spectroscopy (XPS). Their anode performances were investigated by galvanostatic measurement. Furthermore, the effects of the amount of boron dopant and graphitization temperature on the anode performances of boron-doped graphites were also studied.

2. Experimental

2.1. Materials

Shot coke and sponge coke were used in this study, and their compositions of as-received forms are summarized in Table 1.

After grinding into the size of less than 75 μm, shot and sponge cokes were calcined at 1300 °C (abbreviated as SHC13

* Corresponding author. Tel.: +86 10 82338267; fax: +86 10 82338267.
** Corresponding author. Tel.: +81 92 5837801; fax: +81 92 5837798.
E-mail addresses: ryluo@buaa.edu.cn (R. Luo), yoon@cm.kyushu-u.ac.jp (S.-H. Yoon).

0378-7753/$ – see front matter © 2009 Elsevier B.V. All rights reserved.
doi:10.1016/j.jpowsour.2009.08.104

Table 1
Industrial analysis and elemental analysis of as-received shot and sponge cokes (wt.%).

Cokes	Fixed carbon	Volatile	Ash	Water	C	H	N	Diff.
SHC	88.74	11.08	0.18	1.26	88.54	3.93	3.06	4.47
SPC	89.26	10.21	0.53	5.40	90.09	3.66	2.31	3.94

and SPC13, respectively), and then were graphitized at 2400 and 2800 °C, respectively, under Ar atmosphere (abbreviated as SHC24, SHC28, SPC24 and SPC28). Boric acid powder (H_3BO_3) was mixed with SHC13 and SPC13 by 20 wt.%, respectively, and then were heat-treated at 800 °C for 1 h under Ar atmosphere, followed by graphitization at 2800 °C under Ar atmosphere (abbreviated as SHCB28-2 and SPCB28-2, respectively). To investigate the effect of the amount of boron dopant on the anode performances of the resultant boron-doped graphites, H_3BO_3 was also mixed with SHC13 by 10 and 30 wt.% followed by the same treatment as SHCB28-2, and the resultant boron-doped graphites were abbreviated as SHCB28-1 and SHCB28-3. SHCB24-2/SPCB24-2 was prepared by graphitizing the mixture of SHC13/SPC13 and 20 wt.% H_3BO_3 at 2400 °C to compare with SHCB28-2/SPCB28-2.

2.2. Characterization of samples

The microtexture of the prepared samples was studied by a scanning electron microscope (SEM; JSM-6700F JEOL, Japan). The crystallographic data were collected using an X-ray diffractometer (Ultima III Rigaku, Japan) with Cu Kα (λ = 0.15406 nm) radiation, and the crystallographic parameters were calculated according to the revised Gakushin method [21]. The standard silicon powder (200 Mesh, 99.99%, Soekawa Chemical Co., Japan) was mixed with each sample to be measured by 10 wt.% as an internal standard. The chemical state of boron and carbon in the boron-doped samples was analyzed using an X-ray photoelectron spectroscopy (JPS-9010MC JEOL, Japan) with Mg Kα radiation (1253.6 eV). The C 1s peak of carbon was used as a reference for the chemical shift determination, assuming that its binding energy is 284.2 eV.

2.3. Measurement of anode performance

Test electrode was fabricated by spreading a slurry mixture of active material (90 wt.%) and PVdF (polyvinylidene fluoride, 10 wt.%) dissolved in NMP (1-methyl-2- pyrrolidone) solution onto the copper foil, and rolling it after drying under vacuum for 12 h at 120 °C. Two-electrode test cell was assembled by using lithium foil as the counter electrode, 1 M $LiPF_6$ in EC/DEC (1:1, v/v) as the electrolyte and polyethylene film as the separator. The cell assembly was carried out in an argon-filled glove box.

Electrochemical evaluation was performed using TOSCAT-3100 battery testing unit (TOYO SYSTEM CO. LTD., Japan). The carbon electrodes were first charged from open circuit voltage to 0 V at 30 mA g^{-1}, and then constant voltage (CV) charging was applied at 0 V until current decreased to 3 mA g^{-1}. Constant current (CC) discharging was performed at 30 mA g^{-1} until 2 V.

3. Results

3.1. Characterization of as-prepared samples

Fig. 1 shows SEM images of as-received shot and sponge cokes, SHCB28-2 and SPCB28-2. Microtexture of cokes evidently changes from bulky form to a highly developed plate-like texture with parallel alignment of the layers. Compared with boron-doped graphite from sponge coke, more byproducts, which are boron carbide according to XRD and XPS results later, are observed on the surface of boron-doped graphite from shot coke.

Fig. 2 shows XRD patterns of graphitized shot and sponge cokes and boron-doped graphites. As graphitization temperature increases, the (0 0 2), (0 0 4) and (0 0 6) peaks shift to a higher diffraction angle, in corresponding to the decrease of interlayer spacing, d_{002}. The (1 0 1), (1 0 3) and (1 1 2) peaks become clearer, which indicate a more developed three-dimensional stacking layer structure of graphite. Compared with undoped samples, boron-doped samples also show a similar tendency in spite of the same graphitization temperature. It implies improvement of graphite crystallinity with boron doping. In addition, the peaks attributed to B_4C are observed in the range of 30–40° for SHCB28-2, while they do not appear in XRD pattern of SPCB28-2, which is in consistence with their SEM images.

The calculated lattice sizes of as-prepared samples are shown in Table 2. Boron-doped sample shows a lower d_{002} and a growth in crystallite thickness ($L_{c(002)}$) and lattice constant (a_0). The decrease of d_{002} is thought to be related to the depleted p-electrons between graphite layers [13]. The increase of a_0 is because B–C bond caused

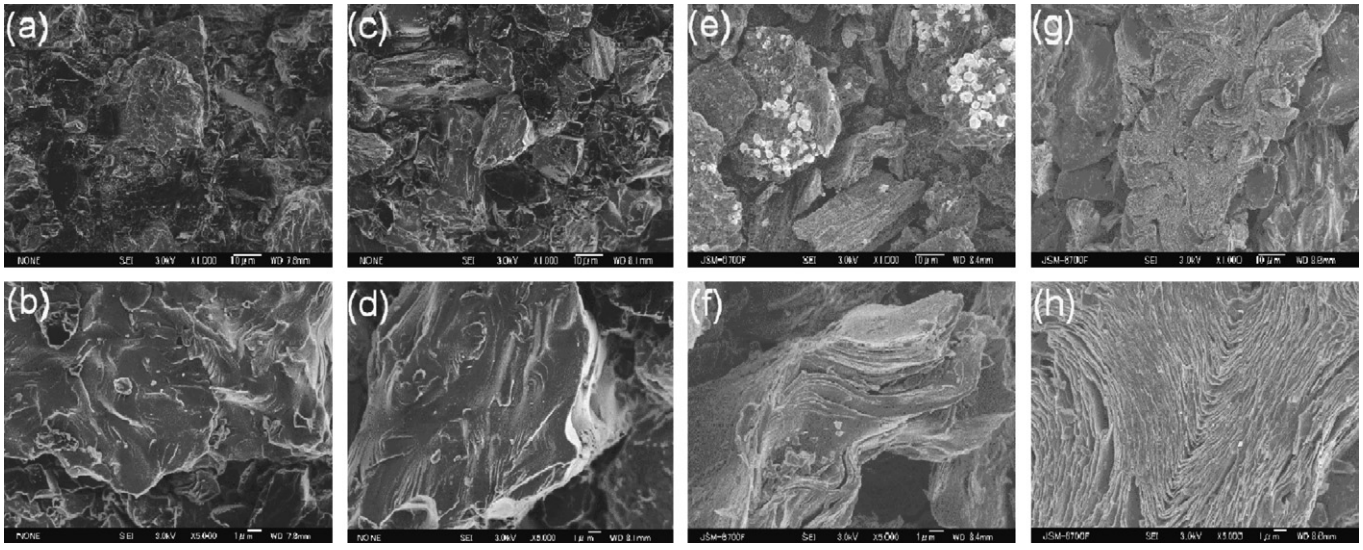

Fig. 1. Low and high magnification SEM images of as-received shot coke (a and b), as-received sponge coke (c and d), boron-doped shot coke (e and f) and boron-doped sponge coke (g and h) graphitized at 2800 °C.

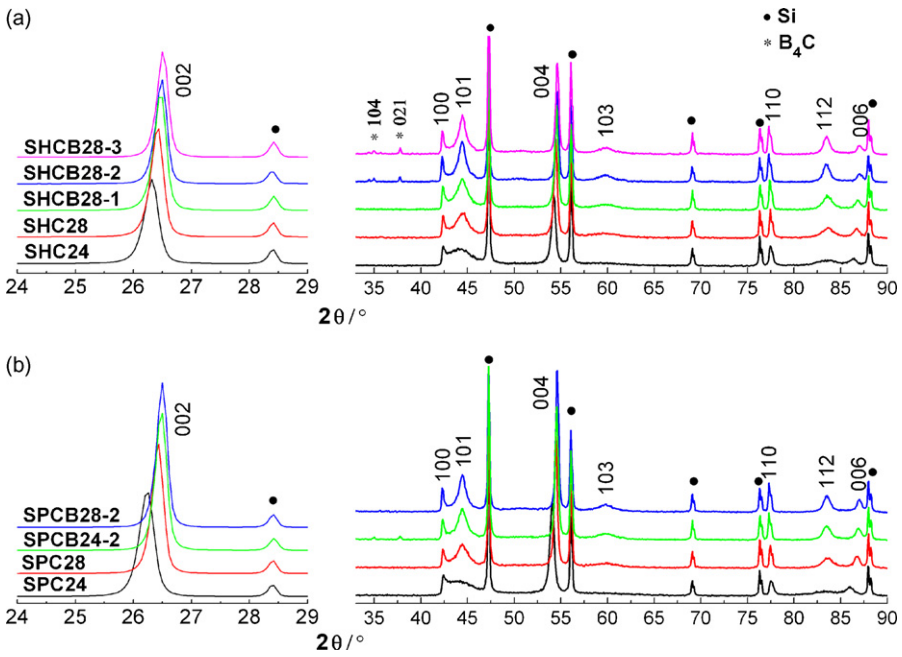

Fig. 2. XRD patterns of graphitized and boron-doped shot (a) and sponge (b) cokes.

by boron atom substituted in the carbon lattice had a longer bond length than C–C bond. It supports the result calculated through molecular simulation method by Endo et al. [8]. Furthermore, a_0 monotonously increases with an increasing amount of boron-containing compound, which indicates more substituted boron atoms. On the other hand, for shot coke, the crystallite width ($L_{a(110)}$) of boron-doped sample is lower than that of undoped sample, while for sponge coke, $L_{a(110)}$ of the boron-doped sample is higher.

Fig. 3 shows XPS C 1s and B 1s spectra of graphitized shot and sponge cokes and boron-doped graphites. For both types of cokes, C 1s peaks of boron-doped samples are located at a slightly lower binding energy compared with those of boron-undoped samples. The reduction of binding energy of C 1s peak for boron-doped sample might be caused by the reduction of the Fermi level due to the redistribution of π-electrons within the graphite layers [22,23].

As expected, the B 1s peaks appear in boron-doped samples, but their forms and positions are different and determined by the sample, the amount of boron-containing compound added and graphitization temperature. SHCB28-1, similar to SPCB28-2, only has one B 1s peak near 185.7 eV, attributed to boron in boron carbide. While for SHCB28-2 and SHCB28-3, apart from B–C peak, the other B 1s peak is also observed at 187.3 eV, which is assigned to boron substituted in carbon lattice according to the results reported in the previous literature [24]. In addition, when the graphitization temperature increases from 2400 to 2800 °C, B 1s peak attributed to boron substituted in carbon lattice is reduced largely or disappears. It indicates that the substituted boron atom begins to leave its substitutional site above 2400 °C.

Table 2
The calculated lattice size of as-prepared samples (nm).

Sample	$d_{(002)}$	$L_{c(002)}$	$L_{a(110)}$	a_0
SHC24	0.3378	91	65	0.24613
SHC28	0.3367	140	116	0.24613
SHCB28-1	0.3361	158	99	0.24636
SHCB28-2	0.3355	214	83	0.24651
SHCB28-3	0.3356	218	85	0.24654
SPC24	0.3388	81	72	0.24608
SPC28	0.3365	183	91	0.24615
SPCB24-2	0.3360	206	104	0.24649
SPCB28-2	0.3356	225	108	0.24643

3.2. Anode performances of as-prepared samples

Fig. 4 and Table 3 show the first charge/discharge profiles, specific capacities and initial coulombic efficiencies of as-prepared samples. First of all, both cokes calcined at 1300 °C show the charge/discharge characteristic of soft carbon, i.e., small charge capacities in the CV stage and no discharge plateau at around 0.1 V. After graphitization at 2400 °C, definite plateaus in the voltage range 0–0.3 V, like graphite, are observed, although discharge capacities are almost the same as those of calcined cokes. With the increase of graphitization temperature, discharge capacities of cokes are improved. Especially for sponge coke, discharge capacity of SPC28 increases over 70 mAh g^{-1} compared with that of SPC24. For the boron-doped graphites, both of them obtain discharge capacity of about 350 mAh g^{-1} and initial coulombic efficiency above 90%. The increase of discharge capacities is because of a well developed graphite crystallinity caused by boron doping.

To better understand the effect of boron doping in carbon materials, differential capacitance (dQ/dV) plots for the first and second charge/discharge cycles are shown in Fig. 5. For SHC13 and SPC13, only peak A corresponding to the discharge plateau at ca. 0.05 V, as shown in Fig. 4, can be observed, while for cokes graphitized over 2400 °C, four peaks can be obviously observed. Their charge and discharge dQ/dV plots are basically corresponding to each other, and the corresponding peak is labeled with the corresponding capital and lowercases. In charge, the peaks in the dQ/dV plots for the second cycle shift to a higher potential compared with the peaks in the dQ/dV plots for the first cycle, and peak D is more evident. In discharge, the peaks in the dQ/dV plots for the first and second cycles are basically superposed. Peaks B, C and E can be observed with cokes graphitized at 2800 °C, and they correspond to the discharge plateaus at ca. 0.1, 0.14 and 0.22 V in Fig. 4, respectively. These three peaks are commonly observed with graphite, and they are assigned based on the literature to a coexistence of stages 1 and 2, a coexistence of stages 2 and 2L (liquid-like stage 2) and a coexistence of stages 4 and 1′ (dilute stage 1), respectively. Peak D, accounted as

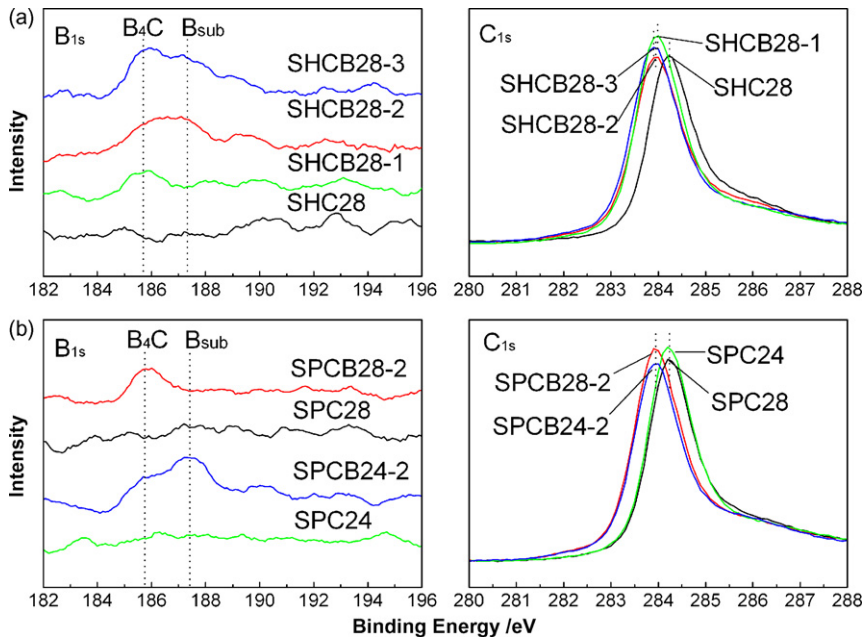

Fig. 3. XPS B 1s and C 1s spectra of graphitized and boron-doped shot (a and b) and sponge (c and d) cokes.

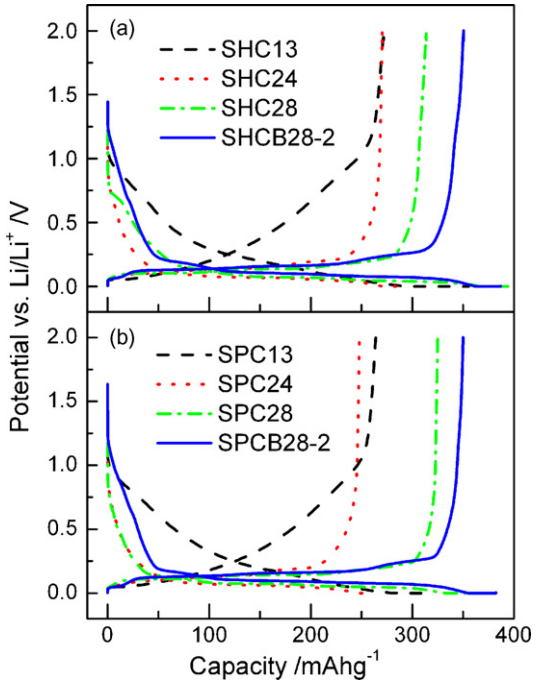

Fig. 4. The first charge/discharge profiles of calcined, graphitized and boron-doped shot (a) and sponge (b) cokes.

intercalation into turbostratic disordered layers [4], is observed in the discharge profile of graphitized cokes. Furthermore, intensity of peak D reduces with the increase of graphitization temperature, and disappears in boron-doped graphites. It indicates that the degree of graphitization increases in the sequence of cokes graphitized at 2400 °C, cokes graphitized at 2800 °C and boron-doped cokes graphitized at 2800 °C, which is in consistence with the result of XRD. On the other hand, the peaks of boron-doped graphites are located at a higher potential compared with the corresponding peaks of graphitized cokes except peak A.

It is interesting to note that a well distinct peak A appears at ca. 0.06 V in the dQ/dV plots of cokes graphitized at 2400 °C and boron-doped graphites. This peak commonly corresponds to Li ion stored in the site to be void-like spaces. This kind of site is supposed to be produced by "molecular bridging" between the edge sites of graphene layer stack with a release of boron atoms substituted at the edge of graphene layer. Furthermore, with the increase of the heat-treatment temperature, such molecular bridging is expected to further proceed to ultimately produce isolated voids or interlayer spaces [25]. Therefore, peak A observed in the dQ/dV plots of cokes graphitized at 2400 °C cannot be observed in the dQ/dV plots of cokes graphitized at 2800 °C. However, for the boron-doped graphites, when the graphitization temperature is higher than 2400 °C, as mentioned above, the substituted boron atom begins to leave its substitutional site, especially for the substituted boron atom existing at the edge of graphene layer, thus forms the Li ion storage site corresponding to peak A.

Fig. 6 shows the first charge/discharge profiles of graphitized shot cokes mixed with different amount of boron-containing compound. In spite of different mixing ratio, the resultant boron-

Table 3
Specific capacities and initial coulombic efficiencies of as-prepared samples.

Sample	Specific capacities (mAh g^{-1})		Coulombic efficiency (%)	Sample	Specific capacities (mAh g^{-1})		Coulombic efficiency (%)
	Charge	Discharge			Charge	Discharge	
SHC13	355.5	271.6	76.4	SPC13	322.2	263.8	81.9
SHC24	285.8	270.3	94.6	SPC24	261.3	247.9	94.9
SHC28	396.4	313.7	79.1	SPC28	352.6	324.9	92.1
SHCB28-2	387.0	350.3	90.5	SPCB28-2	382.3	350.0	91.6

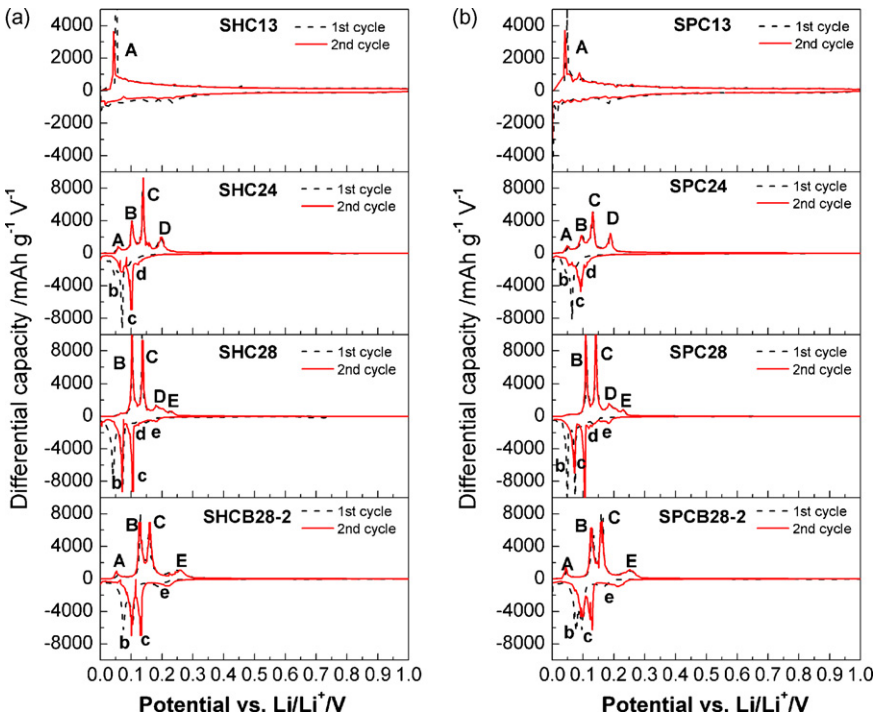

Fig. 5. Differential capacitance (d*Q*/d*V*) plots for the first and second charge/discharge cycles of calcined, graphitized and boron-doped shot (a) and sponge (b) cokes.

doped graphites have the same discharge capacities in the range of 0–0.4 V. Nevertheless, with the increasing amount of boron-containing compound, charge/discharge plateaus shift toward a higher potential, because the presence of substituted boron strengthens the chemical bond between the intercalated Li and the boron–carbon host compared to the pure carbon host [1]. In addition, the initial coulombic efficiency is reduced with the increase of mixing ratio, due to the increasing amount of B_4C formed, which is inactive for Li ion intercalation.

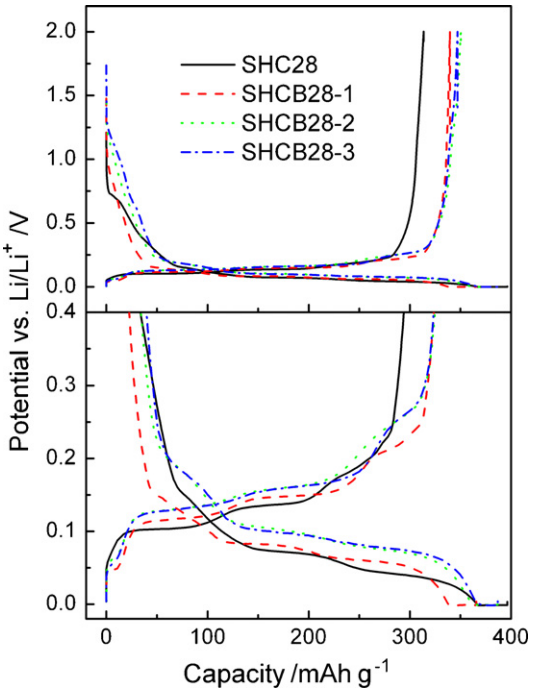

Fig. 6. The first charge/discharge profiles of boron-doped shot cokes with different amount of boron dopant graphitized at 2800 °C.

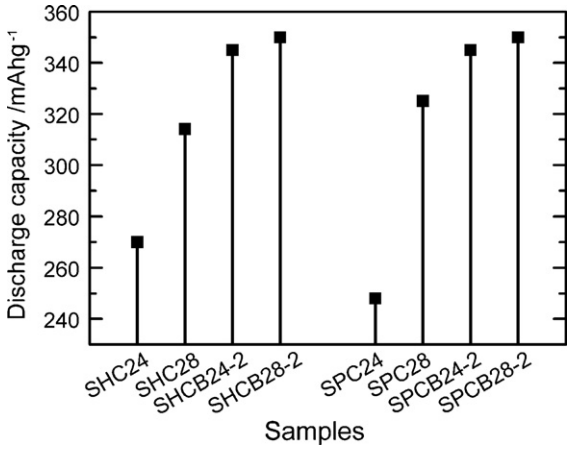

Fig. 7. The relationship between discharge capacity and graphitization temperature of boron-doped cokes.

Fig. 7 shows the relationship between discharge capacity and graphitization temperature of boron-doped cokes. Discharge capacity of SHCB24-2 and SPCB24-2 are only smaller for about 5 mAh g^{-1} than that of SHCB28-2 and SPCB28-2, but larger than that of SHC28 and SPC28. It means that boron doping makes cokes even graphitized at 2400 °C obtain a perfect graphite crystal structure. Therefore, graphitization temperature of synthetic graphite can be decreased from over 2800 to 2400 °C by boron doping. The reduction of electric power consumption caused by this is favorable to reduce the preparation cost of anode material.

4. Conclusion

Boron-doped graphites have been prepared from shot and sponge cokes by mixing with boric acid in this study, and they show obvious plate-like structure. High degree of graphitization was obtained by the substituted boron atom in the carbon lattice. Boron in the resultant boron-doped graphites mainly exist in the

form of boron carbide and boron substituted in the carbon lattice according to the result of XPS measurement.

Both of boron-doped graphites from shot and sponge cokes obtained discharge capacity of 350 mAh g^{-1} and initial coulombic efficiency above 90%. Apart from commonly observed discharge plateau for graphite, boron-doped samples in this study also showed a small plateau at ca. 0.06 V, which is correspond to Li ion storage site to be void-like spaces that are produced by "molecular bridging" between the edge sites of graphene layer stack with a release of boron atoms substituted at the edge of graphene layer. With the increasing amount of boron-containing compound, charge/discharge curves shift toward the higher potential, and initial coulombic efficiency is reduced due to the increasing amount of B_4C. On the premise of near discharge capacity, graphitization temperature of synthetic graphite can be decreased from over 2800 to 2400 °C by boron doping.

In conclusion, boron-doped graphite from shot and sponge cokes is attractive for its application to anode materials for Li ion battery due to its low cost.

References

[1] S. Flandrois, B. Simon, Carbon 37 (1999) 165–180.
[2] M. Endo, C. Kim, K. Nishimura, T. Fujino, K. Miyashita, Carbon 38 (2000) 183–197.
[3] M. Noel, V. Suryanarayanan, J. Power Sources 111 (2002) 193–209.
[4] S.-H. Yoon, C.-W. Park, H.-J. Yang, Y. Korai, I. Mochida, R.T.K. Baker, N.M. Rodriguez, Carbon 42 (2004) 21–32.
[5] T.D. Tran, L.M. Spellman, W.M. Goldberger, X. Song, K. Kinoshita, J. Power Sources 68 (1997) 106–109.
[6] A. Satoh, N. Takami, T. Ohsaki, Solid State Ionics 80 (1995) 291–298.
[7] B.M. Way, J.R. Dahn, J. Electrochem. Soc. 141 (1994) 907–912.
[8] M. Endo, C. Kim, T. Karaki, T. Tamaki, Y. Nishimura, M.J. Matthews, S.D.M. Brown, M.S. Dresselhaus, Phys. Rev. B 58 (1998) 8991–8996.
[9] E. Kim, I. Oh, J. Kwak, Electrochem. Commun. 3 (2001) 608–612.
[10] M.H. Chen, G.T. Wu, G.M. Zhu, J.K. You, Z.G. Lin, J. Solid State Electrochem. 6 (2002) 420–427.
[11] C. Kim, K. Nishimura, T. Fujino, K. Miyashita, M. Endo, M.S. Dresselhaus, J. Electrochem. Soc. 147 (2000) 1257–1264.
[12] C. Kim, T. Fujino, T. Hayashi, M. Endo, M.S. Dresselhaus, J. Electrochem. Soc. 147 (2000) 1265–1270.
[13] M. Endo, C. Kim, T. Karaki, Y. Nishimura, M.J. Matthews, S.D.M. Brown, M.S. Dresselhaus, Carbon 37 (1999) 561–568.
[14] T. Morita, N. Takami, Electrochim. Acta 49 (2004) 2591–2599.
[15] U. Tanaka, T. Sogabe, H. Sakagoshi, M. Ito, T. Tojo, Carbon 39 (2001) 931–936.
[16] H. Fujimoto, A. Mabuchi, C. Natarajan, T. Kasuh, Carbon 40 (2002) 567–574.
[17] T. Hamada, K. Suzuki, T. Kohno, T. Sugiura, Carbon 40 (2002) 2317–2322.
[18] E. Frackowiak, K. Kierzek, G. Lota, J. Machnikowski, J. Phys. Chem. Solids 69 (2008) 1179–1181.
[19] H. Marsh, C. Calvert, J. Bacha, J. Mater. Sci. 20 (1985) 289–302.
[20] D.A. Tillman, N.S. Harding, Fuels of Opportunity, Elsevier, New York, 2004.
[21] N. Iwashita, C.-R. Park, H. Fujimoto, M. Shiraishi, M. Inagaki, Carbon 42 (2004) 701–705.
[22] G. Henning, J. Chem. Phys. 42 (1965) 1167–1172.
[23] L.E. Jones, P.A. Thrower, Carbon 29 (1991) 251–269.
[24] J.S. Burgess, C.K. Acharya, J. Lizarazo, N. Yancey, B. Flowers, G. Kwon, T. Klein, M. Weaver, A.M. Lane, C.H. Turner, S. Street, Carbon 46 (2008) 1711–1717.
[25] C.-W. Park, S.-H. Yoon, S.-I. Lee, S.-M. Oh, Carbon 38 (2000) 995–1001.